NMR structures of a mitochondrial transit peptide from the green alga *Chlamydomonas reinhardtii*

Jean-Marc Lancelin[a,b,*], Pierre Gans[a], Eftychia Bouchayer[a], Isabelle Bally[a], Gérard J. Arlaud[a], Jean-Pierre Jacquot[c]

[a]*Institut de Biologie Structurale CEA-CNRS, 41, Avenue des Martyrs, F-38027 Grenoble, France*
[b]*Laboratoire de RMN Biomoléculaire associé au CNRS, Bâtiment 308, Université Claude Bernard, Lyon I and Ecole Supérieure de Chimie Physique et Electronique de Lyon, F-69622 Villeurbanne, France*
[c]*Laboratoire de Physiologie Végétale Moléculaire, Bâtiment 630, Unité Associée au CNRS 1128, Université de Paris-Sud, F-91405 Orsay, France*

Received 28 May 1996; revised version received 26 June 1996

Abstract The 26-amino-acid pre-sequence of the ATP synthase β subunit that directs the protein from the cytosol to mitochondria in the unicellular green alga *Chlamydomonas reinhardtii* has been synthesised and analysed using NMR spectroscopy/circular dichroism and compared to a chloroplast transit peptide from the same organism. The results demonstrate that the peptide, though mainly unstructured in water, undergoes a strong conformational change in a 36% water/64% 2,2,2-trifluoroethanol mixture. In this solvent condition, an α-helix was characterised by NMR from residue 2 to 26. Structure calculations under NMR restraints lead to a population of models of which 60% are kinked at position 9–10. Structural analysis indicates two hydrophobic sectors on the models with a discontinuity at the 9–10 kink level. The structures suggest a different interaction mode with the mitochondrial membrane compared to the chloroplast transit peptide.

Key words: Mitochondrial protein import; Transit peptide; ATP synthase; Peptide synthesis; NMR structure; *Chlamydomonas reinhardtii*

1. Introduction

Mitochondrial and chloroplastic proteins that are encoded at the nuclear level are expressed in the cytosol with an N-terminal pre-sequence that is sufficient to route them to the corresponding organelle and to trigger an ATP-dependent translocation mechanism through its envelope. Although the selective protein uptake by these organelles is encoded by the protein pre-sequence, no consensus sequences have been identified in the transit peptides. We recently described the conformational properties of the isolated synthetic 32-amino-acid pre-sequence from the chloroplastic ferredoxin of the eukaryotic green alga *Chlamydomonas reinhardtii* [1]. In particular, we showed that 2,2,2-trifluoroethanol (TFE), known to mimic the conformational change induced by biomembranes on transit pre-sequences, causes the stabilisation of an α-helix restricted to residues 3–13, while the remainder of the peptide is randomly distributed on the side opposite to a hydrophobic ridge formed by Met-5, Phe-9 and Val-13 on the induced α-helix. These data suggested to us a possible surface interaction between the membrane of the organelle and the inducible α-helix, while the unstructured C-terminal part would remain available for further interaction with the proteins involved in the chloroplast translocation machinery.

A comparative study on mitochondrial transit peptide (mTP) taken from the same organism may, therefore, help in understanding how the routing specificity is encoded by the transit sequence. The mTP of the ATP synthase β subunit is one of the three mTPs described in *C. reinhardtii* [2–4]. This mTP was prepared by solid-phase peptide synthesis and analysed under conditions similar to those used in our previous study. The calculated structures, based on 150 geometric boundaries derived from NMR data in 36% H_2O/64% CF_3CD_2OD at 20°C, are discussed in terms of potential interactions with the mitochondrial envelope and its molecular translocation machinery.

2. Materials and methods

2.1. Peptide synthesis

The ATP synthase β-subunit mTP was synthesised chemically by the stepwise solid-phase method [5], using an Applied Biosystems 430A automated synthesiser. Synthesis was performed on a phenylacetamidomethyl resin, and the *t*-butyloxycarbonyl group was used for protection of the *N*-α-amino group of all amino acids. Protecting groups for amino acid side chains were as follows: Arg (mesitylene sulfonyl), Ser (benzyl), Thr (benzyl), and Lys (2-chlorobenzyloxycarbonyl). Met was used without side chain protection. All couplings were performed by the dicyclohexylcarbodiimide/1-hydroxybenzotriazole method, using *N*-methylpyrrolidone and dimethylsulfoxide as coupling solvents, according to the protocol defined by Applied Biosystems. Except for Gly, all amino acids were double coupled, and amino groups left unreacted after each coupling cycle were capped with acetic anhydride.

Deprotection and cleavage of the peptide from the resin was performed with trifluoromethanesulfonic acid. Reduction of methionine sulfoxide generated during synthesis was achieved by treatment of the peptide with *N*-methyl mercaptoacetamide as described previously [6]. The peptide was purified by preparative reverse-phase HPLC on a 30 nm Vydac C18 column (2.2 cm × 25 cm, 10 μm). Fractions of 50 mg of the peptide dissolved in 6 M guanidine hydrochloride were first loaded onto the column and elution was carried out by means of a linear gradient of 5–60% acetonitrile in 0.1% trifluoroacetic acid. Further purification was achieved on the same column by using isocratic elution with 31% acetonitrile/0.1% trifluoroacetic acid. Analytical separations were performed on a 30 nm Vydac C18 column (0.46 cm × 25 cm, 5 μm) using the gradient system described above. The peptide was detected based on its absorption at 215 nm.

2.2. Electrospray mass spectrometry

Mass spectrometry analyses were performed by the electrospray ionization technique on an API III triple-quadrupole mass spectrometer (PE/Sciex, Thornill, Canada) equipped with a nebulizer-assisted electrospray (ionspray) source, as described previously [7].

*Corresponding author. Fax: (33) 72431395.
E-mail: lancelin@ginko.cpe.fr

Abbreviations: CD, circular dichroism; TFE, 2,2,2-trifluoroethanol; cTP, chloroplastic transit peptide; mTP, mitochondrial transit peptide; rMD, restrained molecular dynamic, R.m.s., root-mean-square; R.m.s.d., R.m.s. deviation.

PII S0014-5793(96)00734-X

2.3. Circular dichroism

Spectra were recorded at 20°C between 190 and 250 nm on a Jobin-Yvon CD6 spectro-dichrograph, using a quartz cell of 1 mm path length, with a 5 s integration time of each 0.5 nm step. For each condition, two spectra were averaged and the baseline was corrected for neat solvents or solvent mixtures. Water-TFE mixtures were obtained by mixing two equivalent solutions of ferredoxin cTP at 110 μg/ml, prepared either in pure bi-distilled water (pH 3.7) or in pure TFE (Aldrich Chemicals Co.).

2.4. NMR measurements

Samples were dissolved at 4 mM concentration in 90% H_2O/10% ^2H_2O and the pH was adjusted to 4.0 at 20°C (direct uncorrected pH-meter reading) by addition of μl increments of 0.1 N NaOH and 0.1 N HCl. A sample in 36% H_2O/64% CF_3CD_2OD (70:30, mol/mol) was obtained from the lyophilisation of a sample in 90% H_2O/10% ^2H_2O (pH 4.0), followed by dissolution in the H_2O/CF_3CD_2OD solvent mixture. In both cases, samples were sealed in a 5 mm diameter NMR tube under argon.

NMR spectra were recorded at 20°C on Bruker AM-X spectrometers operating at 400 and 600 MHz proton frequencies. Chemical shifts were quoted relative to the water resonance fixed at 4.77 ppm at 25°C and at 4.92 ppm at 10°C. ^1H 2D spectra, DQF-COSY (double quantum filtered correlation spectroscopy) [8], TOCSY/HOHAHA (total correlation spectroscopy/ homonuclear Hartmann-Hahn spectroscopy) [9,10], and NOESY (nuclear Overhauser spectroscopy) [11,12] spectra were recorded in the phase-sensitive mode using the hypercomplex method [13]. Water resonance was attenuated by means of a coherent low-power ($\gamma B_2/2\pi = 50$ Hz) presaturation during the relaxation delay. For HOHAHA and NOESY this presaturation was further combined with a 'jump and return' read pulse [14]. The Waltz-17 mixing scheme used in TOCSY/HOHAHA experiments was optimised according to the technique known as clean TOCSY [15]. Two-dimensional spectra were collected as a 512 (t_1) and 1024 (t_2) complex point time-domain matrix using a spectral width of 3400 Hz ($^1H = 400$ MHz) or 5100 Hz ($^1H = 600$ MHz) in both dimensions and 32 scans per t_1 increment. They were transformed after zero-filling in the $F1$ dimension, into 1024 and 1024 real points in $F1$ and $F2$ dimension frequency-domain spectra. HOHAHA spectra were recorded with a mixing time of 45 ms that includes the delays of the clean-TOCSY pulse scheme. NOESY spectra were recorded with 30, 50, 75, 150 and 300 ms mixing times. $^3J_{HN\alpha}$ were evaluated by a combination of direct reading from a one-dimensional spectrum, the compared aspect of Hα-HN COSY cross-peaks, and the efficiency of magnetisation transfer in the HOHAHA spectrum.

2.5. NMR-derived geometrical bounds

From the NOESY spectra (75 and 150 ms mixing times) recorded in 36% H_2O/64% CF_3CD_2OD at 20°C, the relative intensities of NOE cross-peaks were converted as 2.7, 3.3, and 5.0 Å upper-distance boundaries for strong, medium and weak intensities, respectively. The NOE between side-chain $N^{\gamma}H_E$ and $N^{\gamma}H_Z$ amide protons of Asn-16 was used as reference to categorise the NOEs. No lower-distance boundaries were derived from NOEs. An error of 0.3 Å was added to a distance boundary involving an amide proton. The possibility of spin diffusion precludes higher precision in the derivation of distance limits. Methyl, methylene, and aromatic protons that give rise to a single resonance line were treated as a pseudo-atom at their geometric center and the distances were corrected according to the pseudo-structure generated [16]. All other methylene protons were treated individually as floating prochiral pairs. A φ dihedral restraint was applied when the measured $^3J_{HN\alpha}$ value was smaller than 5 Hz ($-65 \pm 25°$) in a recognised helical structure.

2.6. Structure calculations

Structural calculations were performed using the molecular dynamic program DISCOVER (version 2.9) from Biosym Technologies functioning with the AMBER4 force field [17]. The protocol was divided into two parts: In the first stage a simulated annealing procedure was used to provide the broadest possible sampling of the conformational space. Cartesian co-ordinates were randomised at the start of each run. In the initial stages the calculation is dominated by the experimental constraints (force constant for the semi-parabolic distance constraints was 50 kcal mol^{-1} $Å^{-2}$ and 200 kcal mol^{-1} $Å^{-2}$ for the dihedral constraints); experimental, covalent and non-bond terms were augmented gradually during the high-temperature (1000 K) period of the simulation before final cooling to 300 K [18]. The non-bond terms were reduced to a simple repulsive quartic term to facilitate interrogation of a large conformational space and the Coulombic interaction was ignored in this first step. Total simulation time in this first step was 62 ps. These approximate structures were then refined using an rMD calculation using the full AMBER4 force field description (including Coulomb and van der Waals terms). Solvent effects were approximated using reduced charges for the polar residues as described previously [19]. The molecule was equilibrated at a temperature of 600 K, using distance constraints of 25 kcal mol^{-1} $Å^{-2}$ and 100 kcal mol^{-1} $Å^{-2}$ for the dihedral constraints, allowed to evolve during a period of 10 ps and then cooled over a period of 5 ps to 300 K, where the molecule was again allowed to evolve over 15 ps. The step size for the calculation of velocities was 1 fs. Final structures were energy minimised using the same force field with a conjugate gradient algorithm and these structures were used for analysis.

3. Results

Chromatographic analysis of the final synthetic peptide by reverse-phase HPLC indicated that it was homogeneous. Electrospray mass spectrometry analysis showed that the peptide had the expected sequence, yielding a mass value of 2765.7 ± 0.4, consistent with the calculated average mass (2765.3). The peptide material contained about 5% of a species with an extra mass of 90, likely arising from reattach-

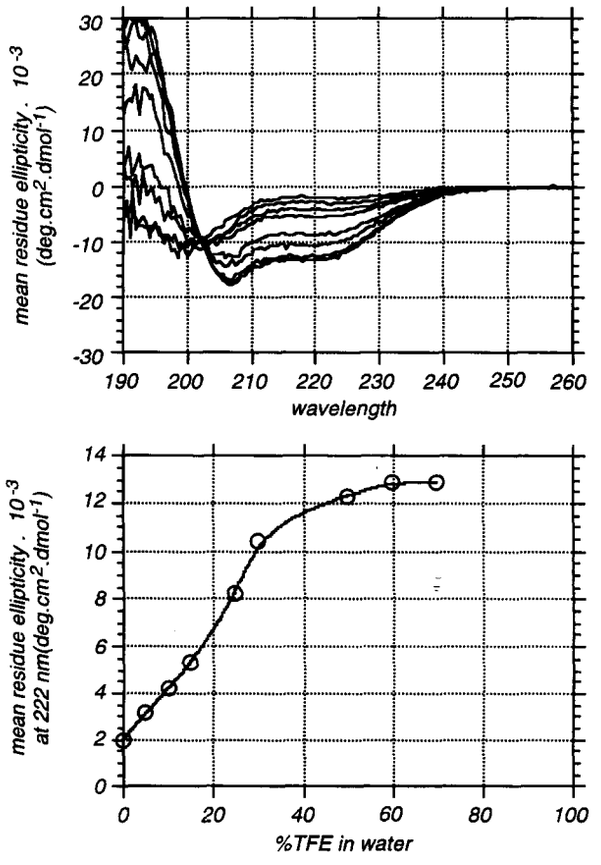

Fig. 1. Far-UV CD spectra of the synthetic *C. reinhardtii* ATP synthase β-subunit mTP in the presence of increasing concentrations of CF_3CH_2OH in water (upper panel). In the lower panel, the absolute value of the mean residue ellipticity at 222 nm is plotted against the CF_3CH_2OH concentration.

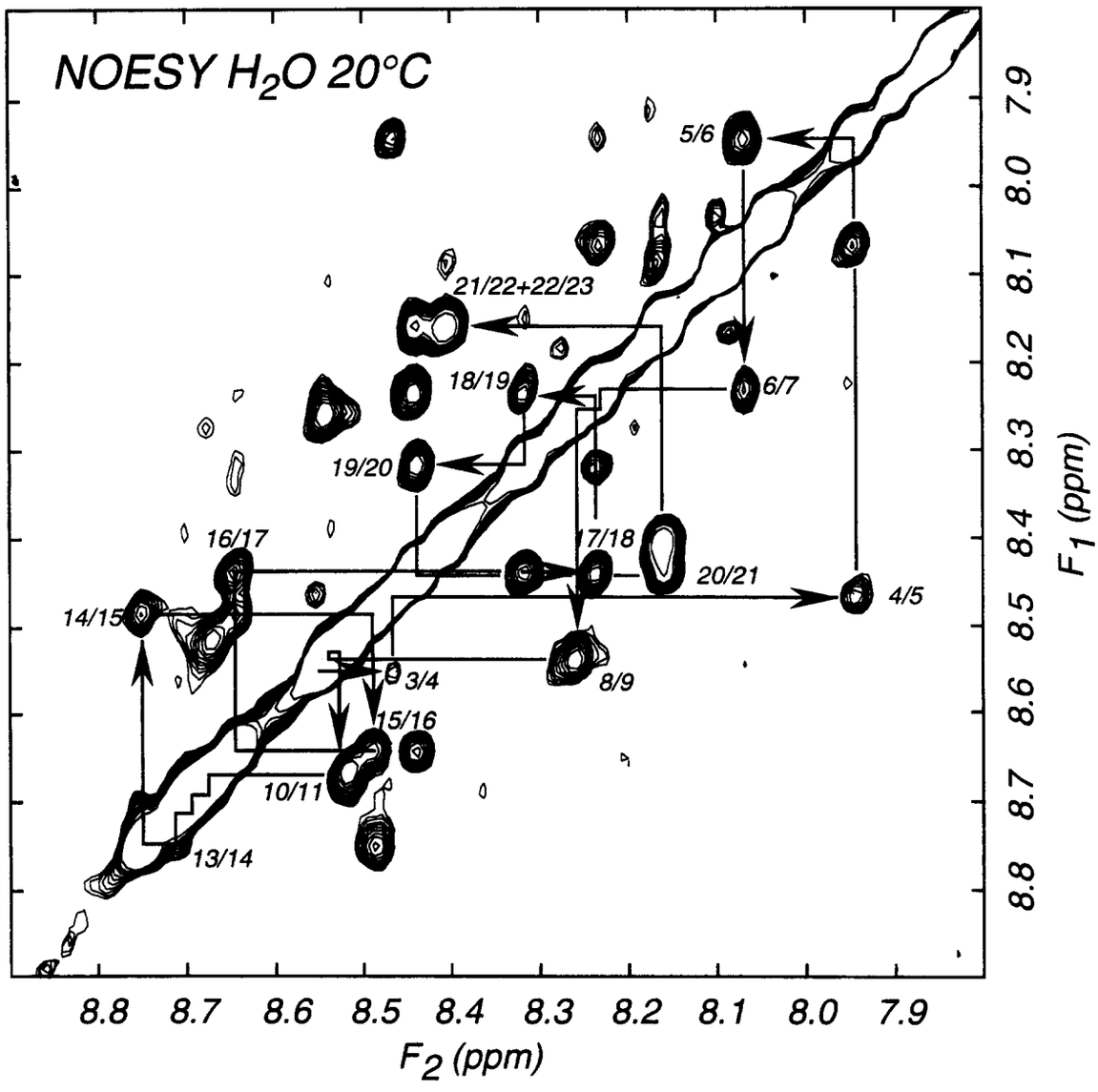

Fig. 2. NH(F_2)-NH(F_1) region of the NOESY spectrum recorded at 600 MHz (150 ms mixing time) of synthetic the *C. reinhardtii* ATP synthase β-subunit mTP (4 mM in 36% H_2O/64% CF_3CD_2OD) at 20°C. Sequential connectivities are arrowed from residue 3 to 22.

ment, during deprotection by trifluoromethanesulfonic acid, of a benzyl protecting group.

Fig. 1 shows CD spectra in the far-UV of *C. reinhardtii* mTP in water and in water-TFE mixtures at 20°C. The spectrum in water exhibits a low mean residue ellipticity at 222 nm (about -2000 degree cm^2 dmol^{-1}), characteristic of a very low helical content. No significant variation was detected at lower or higher temperatures. However, a pronounced increase in the helical content was obtained by adding increasing amounts of TFE. An isodichroic point around 203 nm is indicative of a two-state coil to helix transition. At 60% TFE in water, the mean-residue ellipticity at 222 nm reached a plateau at approx. $-13\,000$ degree cm^2 dmol^{-1}.

The NMR sequence-specific proton assignments [16] were easily obtained either in 90% H_2O/10% ^2H_2O or in 36% H_2O/64% CF_3CD_2OD at 20°C. Fig. 2 shows a representative part of the NOESY spectrum in 36% H_2O/64% CF_3CD_2OD. NOEs as well as $^3J_{HN\alpha}$ spin-spin coupling constant analysis indicated that no significant helical content in pure water could be detected by NMR. Similarly, analysis in 90% H_2O/10% ^2H_2O confirmed the unstructured character of the peptide. In contrast, the same NMR analysis performed in 36% H_2O/64% CF_3CD_2OD, as summarised in Fig. 3, provided strong evidence for α-helix formation. The medium distance NOEs indicate that the helix spans from residues 2 to 26, with most of the missing NOEs being due to accidental spectral overlaps.

From the NMR data obtained in 36% H_2O/64% CF_3CD_2OD, 150 geometrical boundaries, including 12 φ dihedral-angle restraints (Fig. 3), 70 sequential and 47 medium-range upper-bound distances, were deduced and used in the structure calculation procedure. 26 structures that fulfill the structural quality criteria described in Table 1, were calculated. Fig. 4 shows the 26 models superimposed for a minimum backbone R.m.s.d. from residues 3 to 8. In the model ensemble, 11 structures adopt a regular α-helix conformation from residue 2 to 24 and the other 15 models are kinked by a statistical distribution of the Ala-9 backbone ψ angle.

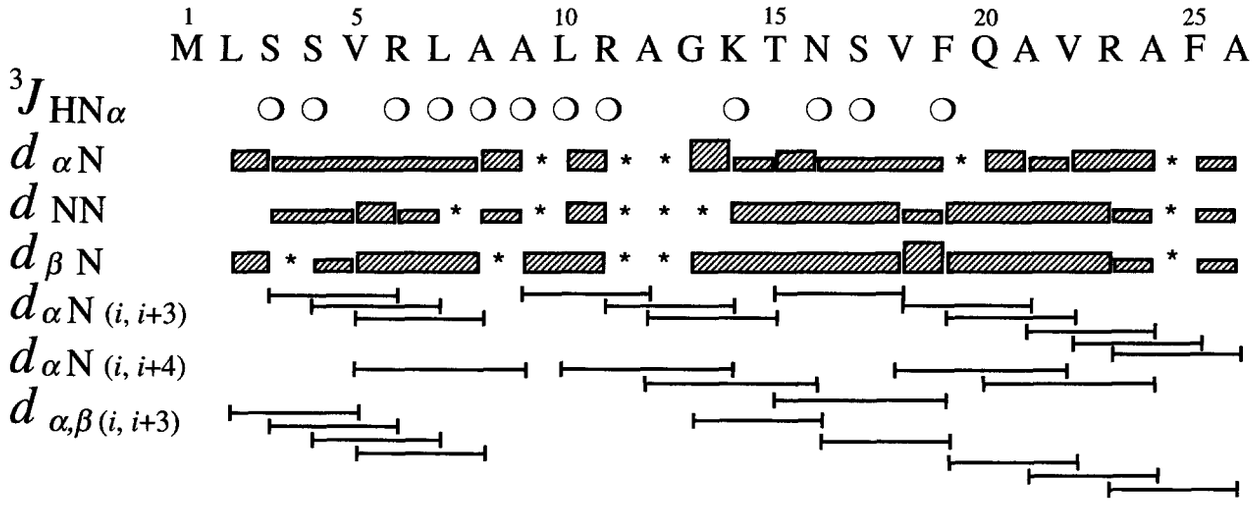

Fig. 3. Summary of the sequential NOE connectivities involving NH, $C^{\alpha}H$ and $C^{\beta}H$ measured at 20°C with 150 ms mixing time in 36% H_2O/64% CF_3CD_2OD. NOEs are classified as strong, medium and weak according to the height of the hatched bar under the peptide sequence. Asterisks indicate a spectral overlap that precludes observation of the NOE. Circles indicate a $^3J_{HN\alpha}$ spin-spin coupling constant measured on one-dimensional spectra at 20°C lower than 5 Hz.

4. Discussion

CD and NMR analysis demonstrate that the *C. reinhardtii* ATP-synthase β-subunit mTP can adopt a helical conformation in water-TFE mixtures while in pure water only CD detected a small helical contribution at 222 nm. Contrary to the ferredoxin chloroplastic transit peptide (cTP) previously analysed by us, the helix induction by TFE starts more quickly (Fig. 1). This indicates a greater propensity of the mTP for adopting the helical conformation. This can also be correlated with the observation that a small helical content was detectable by CD in pure water for mTP in contrast to ferredoxin cTP under the same experimental conditions [1]. The induced helix is also much longer in mTP compared to cTP. The helix spans almost the complete mTP sequence, while helical induction by TFE was only restricted to the N-terminal 5–13 cTP region. However, 15 out of the 26 NMR-derived mTP models are kinked between Ala-9 and Leu-10.

Table 1
Structural statistics for the 26 structures of *C. reinhardtii* ATP synthase β-subunit mTP determined in 36% H_2O/64% CF_3CD_2OD[a]

Structural statistics	26 structures
Cartesian coordinate R.m.s.d. (Å)[b]	
Residues 3–8	0.19 ± 0.25
Residues 11–24	0.22 ± 0.20
Mean number of distance restraints violation per structure[c]	
> 0.3 Å	0
> 0.2 Å	0.08 ± 0.27
> 0.1 Å	0.14 ± 0.45
AMBER potential energies[d]	
E_{Total} (kcal mol^{-1})	−428 ± 15
$E_{Coulombic}$ (kcal mol^{-1})	−394 ± 11
E_{L-J} (kcal mol^{-1})	−56 ± 4

[a]The '26 structures' refer to the final NMR-derived structures.
[b]Mean R.m.s.d were calculated vs the lowest energy structure 26 using (N, C^{α}, C) backbone atoms.
[c]All the NOEs (see text) were used for the statistics.
[d]$E_{Coulombic}$ is the coulombic energy contribution to E_{Total}. E_{L-J} is the value of the Lennard-Jones van der Waals energy function calculated by DISCOVER using the AMBER force-field [17].

Examination of the induced helical structures of mTP shows that they are also amphiphilic but that, in contrast to cTP, there is no continuum in the hydrophobic sector along the helix axis. Indeed, the hydrophobic sector is disrupted at the level where some NMR models kink as shown in Fig. 5. The kink occurs in the NMR models at a position where there is also a discontinuity in the medium distances due to accidental spectral overlaps that precluded the assignment of the corresponding NOEs. Therefore, we cannot rule out that this feature could be artifactual. Nevertheless, the correspondence between the discontinuity of the hydrophobic sector and the structural kink is noteworthy.

The fact that the *C. reinhardtii* mTP is more amphipathic and exhibits a greater helical propensity than the previously studied cTP from the same organism correlates with other observations reported in different biological systems [20]. Indeed, a two-domain inducible helix has been reported recently for the mTPs of yeast cytochrome oxidase subunit IV precursor protein [21,22], rat chaperonin 10 [23], rat malate dehydrogenase [24], and rat liver mitochondrial aldehyde dehydrogenase [25]. The high amphipathicity of mTPs was mostly interpreted as determining their ability to bind specifically to the mitochondrial envelope [21,26]. It is also known [27] that antibacterial peptides of the cecropin family, mammal defensins, frog-skin bioactive peptides such as magainin, and also mellitin from honey-bee venom (all known to act at the biomembrane level under amphiphilic helical conformation), are structurally related to mTPs and cross-activities have been reported [27]. Therefore, the preliminary binding to the outer membrane of the mitochondrial envelope is clearly related to the inducible amphipathic helices of mTPs. In addition to this initial interaction, recent results [28] demonstrate that two proteins, MOM22 and MOM19 from highly purified outer membrane vesicles of *Neurospora crassa*, cooperate to recognise specifically and reversibly the mTP at the membrane surface. The salt sensitivity of the interaction indicates a probable

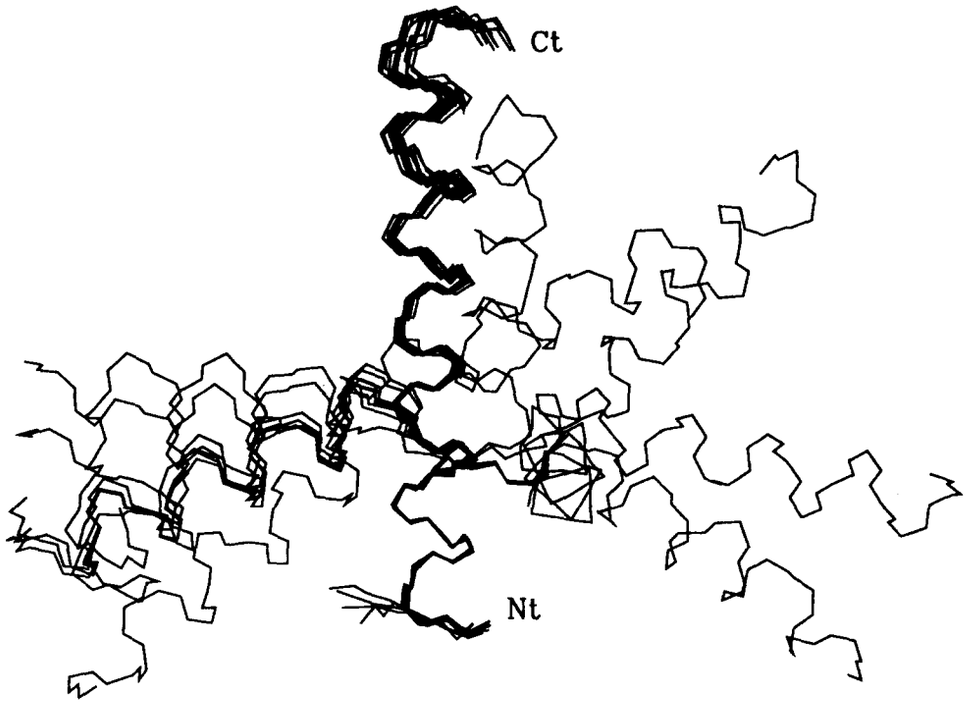

Fig. 4. R.m.s. superpositions of (N, C^{α}, C) atoms from residues 3 to 8 of 26 calculated structures of *C. reinhardtii* ATP synthase β-subunit. Geometrical boundaries were derived from the NMR experiments at 20°C in 36% H_2O/64% CF_3CD_2OD. Only backbone (N, C^{α}, C) atoms have been represented. Nt, N-terminal ends; Ct, C-terminal ends.

electrostatic-dominated interaction between MOM22/19 and the mTP, but other hydrophobic interactions cannot be ruled out. The major conformational differences observed between the two targeting pre-sequences studied in *C. reinhardtii* suggest different interaction with the mitochondrial and chloroplastic translocation protein receptors. For instance, the longer amphipathic helices induced on mTP could be required for an interaction with MOM22/19 occurring deep below the membrane surface. In contrast, the interaction with chloroplast translocation machinery [29,30] could be more surface exposed on the chloroplast outer membrane. *Chlamydomonas* cTPs have been described as sharing features with both mTPs and higher plant cTPs [31]. In addition, 31 amino-terminal residues of a 45-amino-acid cTP in *Chlamydomonas* have been found to direct non-mitochondrial proteins to mitochondria of yeast in vitro [32] with a lower efficiency compared to an authentic yeast mTP. Of course in such a highly artificial system, conclusions cannot be easily drawn, and only a similitude between the mTPs and cTPs function mechanisms was deduced. Our work provides the first structural comparison of a mTP and a cTP in the same organism. This may help us to gain understanding of the molecular mechanisms by which mitochondrial and chloroplast pre-sequences function.

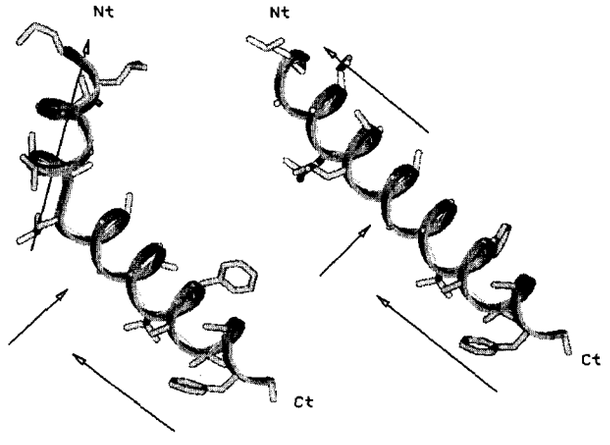

Fig. 5. Two representative NMR models kinked (left) and linear (right) taken from the 26 ensemble of *C. reinhardtii* ATP synthase β-subunit mTP. Side-chains of hydrophobic residues have been represented. The two arrows parallel to the long helix axis indicate the hydrophobic sectors of the amphiphilic structures. The arrows perpendicular to the long helix axis indicate the disruption in the alignment of the hydrophobic sectors.

Acknowledgements: E.B. was a recipient of a DRI fellowship from the Commissariat à l'Energie Atomique. We thank C. Saint Pierre for performing mass spectrometry analyses. Co-ordinates have been deposited at the Protein Data Bank at Broohaven National Laboratory.

References

[1] Lancelin, J.-M., Bally, I., Arlaud, G.J., Blackledge, M.J., Gans, P., Stein, M. and Jacquot, J.-P. (1994) FEBS Lett. 343, 261–266.
[2] Nurani, G and Franzén L.-G. (1996) Plant Mol. Biol., in press.
[3] Atteia, A. and Franzén L.-G. (1996) Eur. J. Biochem., in press.
[4] Franzén, L.-G. and Falk, G. (1992) Plant Mol. Biol. 19, 771–780.
[5] Tam, J.P., Heath, W.F. and Merrifield, R.B. (1983) J. Am. Chem. Soc. 105, 6442–6445.
[6] Girardet, J.-L., Bally, I., Arlaud, G.J. and Dupont, Y. (1993) Eur. J. Biochem. 217, 225–231.
[7] Petillot, Y., Thibault, P., Thielens, N.M., Rossi, V., Lacroix, M., Coddeville, B., Spik, G., Schumaker, V.N., Gagnon, J. and Arlaud, G.J. (1995) FEBS Lett. 358, 323–328.
[8] Rance, M., Sørensen, O.W., Bodenhausen, G., Wagner, G., Ernst, R.R. and Wüthrich, K. (1983) Biochem. Biophys. Res. Commun. 117, 479–485.
[9] Braunschweiler, L. and Ernst, R.R. (1983) J. Magn. Reson. 53, 521–528.

[10] Davis, D.G. and Bax, A. (1985) J. Am. Chem. Soc. 107, 2820–2821.
[11] Jeener, J., Meier, B.H., Bachmann, P. and Ernst, R.R. (1979) J. Chem. Phys. 71, 4546–4553.
[12] Macura, S., Hyang, Y., Suter, D. and Ernst, R.R. (1981) J. Magn. Reson. 43, 259–281.
[13] States, D.J., Haberkorn, R.A. and Ruben, D.J. (1982) J. Magn. Reson. 48, 286–292.
[14] Plateau, P. and Guéron, M. (1982) J. Am. Chem. Soc. 104, 7310–7311.
[15] Griesinger, C., Otting, G., Wüthrich, K. and Ersnt, R.R. (1988) J. Am. Chem. Soc. 110, 7870–7872.
[16] Wüthrich, K. (1986) NMR of Protein and Nucleic Acids, Wiley, New York.
[17] Pearlman, D.A., Case, D.A., Caldwell, J.C., Seibel, G.L., Singh, U.C., Weiner, P. and Kollman, P.A. (1991) AMBER 4.0, University of California, San Francisco, CA.
[18] Nilges, M., Clore, M. and Gronenborn, A. (1988) FEBS Lett. 239, 129–135.
[19] Blackledge, M.J., Medvedeva, S., Poncin, M., Guerlesquin, F., Bruschi, M. and Marion, D. (1995) J. Mol. Biol. 245, 661–681.
[20] Von Heijne, G., Steppuhn, J. and Herrmann, R.G. (1988) Eur. J. Biochem. 180, 535–545.
[21] Chupin, V., Leehouts, J.M., De Kroon, I.P.M. and De Kruijff (1996) Biochemistry 35, 3141–3146.
[22] Endo, T., Shimada, I., Roise, D. and Inagaki, F. (1989) J. Biochem. (Tokyo) 106, 396–400.
[23] Jarvis, J.A., Ryayn, M.T., Hoogenraad, N.J., Craik, D.J. and Høj, P.B. (1995) J. Biol. Chem. 270, 1323–1331.
[24] MacLachlan, L.K., Haris, P.I., Reid, D.G., White, J., Chapman, D., Lucy, J.A. and Austen, B.M. (1994) Biochem. J. 303, 657–662.
[25] Thornton, K., Wang, Y., Weiner, H. and Gorenstein, D.G. (1993) J. Biol. Chem. 268, 19906–19914.
[26] Hammen, P.K., Gorenstein, D.G. and Weiner, H. (1996) Biochemistry 35, 3772–3781.
[27] Hugosson, M., Andreu, D., Boman, H.G. and Glaser, E. (1994) Eur. J. Biochem., 1027–1033.
[28] Mayer, A., Nargang, F.E., Neupert, W. and Lill, R. (1995) EMBO J. 14, 4204–4211.
[29] Schnell, D.J., Kessler, F. and Blobel, G. (1994) Science 266, 1007–1012.
[30] Perry, S.E. and Keegstra, K. (1994) Plant Cell 6, 93–105.
[31] Franzèn, L.-G., Rochaix, J.-D. and Von Heijne G. (1990) FEBS Lett. 260, 165–168.
[32] Hurt, E.C., Soltanifar, N., Goldschmidt-Clermont, M., Rochaix, J.-D. and Schatz, G. (1986) EMBO J. 5, 1343–1350.